

Physical properties of new $\text{Sb}_2\text{O}_3\text{-V}_2\text{O}_5\text{-K}_2\text{O}$ glasses

Y. TAIBI^a, M. POULAIN^b, R. LEBULLENGER^b, L. ATOUTI^a, M. LEGOUERA^c

^aLaboratoire de Métallurgie et Génie des Matériaux, Université de Annaba, 12 Sidi Amar Annaba, Algérie

^bSciences Chimiques, Université de Rennes 1, Campus Beaulieu, F-35042 Rennes, France

^cDept Mécanique, Université de Skikda, 21000 Algérie.

New heavy metal oxide glasses have been prepared and the compositional limits have been investigated in the $\text{Sb}_2\text{O}_3\text{-V}_2\text{O}_5\text{-K}_2\text{O}$ ternary system. Chemical composition of glass samples was checked by EDS analysis. The influence of the $\text{V}_2\text{O}_5/\text{Sb}_2\text{O}_3$ substitution on the physical properties of the $(70-x)\text{Sb}_2\text{O}_3\text{-}x\text{V}_2\text{O}_5\text{-}30\text{K}_2\text{O}$ glasses has been studied in the $0 < x < 40$ range. Density decreases linearly from 4.3 g cm^{-3} to 3.4 g cm^{-3} as V_2O_5 replaces Sb_2O_3 . However, the evolution of the physical properties such as glass transition temperature, elastic modulus, thermal expansion and microhardness is not monotonous. T_g increases for $0 < x < 5$, but it decreases for $x > 5$ with a minimum value between 25% and 35% V_2O_5 . This unusual behavior suggests changes in the coordination number of the vanadium cations in relation to the network topology.

(Received November 27, 2008; accepted January 21, 2009)

Keywords: Vanadate glass, Glass transition, Density, Elastic moduli, Thermal expansion, Microhardness

1. Introduction

Numerous studies have been implemented on vanadium containing glasses [1-31]. While V_2O_5 was considered as a potential glass former in the early paper of Zachariassen[32], various vanadate glasses have been reported in which vanadium oxide was associated to alkali cations[1,16], or divalent metals[33] such as Mg[24], Ca[30], Sr[14], Ba[2] and Pb[12,17,22]. In addition, binary and multicomponent glasses have been synthesized with V_2O_5 and P_2O_5 [4,11,13], B_2O_3 [3,13,19,31], GeO_2 [7] and As_2O_3 [20] as major glass formers. More recently, tellurovanadate glasses have been the subject of numerous studies [6,15,21,26,29, 34-36].

As pointed out by Zachariassen [32], antimony oxide Sb_2O_3 is also a glass progenitor. While this single oxide has been reported to exist in the vitreous form [5,37,38], various binary and multicomponent glasses are obtained by the addition of alkali oxides[39-40]. Since the pioneering work of Portier and Dubois [41-42], numerous oxyhalide glasses based on Sb_2O_3 have been studied [43-45]. Such glasses are often referred to as antimonate glasses, although this name should rather concern compounds based on antimony(V) oxide Sb_2O_5 .

Apart from infrared transmission, semi-conducting properties makes the major interest of vanadium-rich glasses. The conduction mechanism has been understood by small polaron hopping (SPH) model [11,30,31,46]. The hopping of electrons existing in the glass network accompanies a valence change between V^{4+} and V^{5+} in glasses. As in crystalline compounds, lower oxidation states (e.g. V^{3+}) are likely to exist in the glassy state[20].

In the view of the respective positions of Te and Sb in the periodic chart – Te^{4+} and Sb^{3+} have the same

electronic structure- one may expect similarities between the physical properties of tellurite and antimonite glasses. Both have low phonon energy and refractive index in excess of 2. Tellurites exhibit large non-linear optical susceptibility ($\chi^{(3)}$) coefficient[47] and this has also been reported for antimonites[48]. This makes them suitable for applications in non linear optical devices (e.g. ultra fast optical switches and power limiters) and broad band optical amplifiers operating around $1.5 \mu\text{m}$ [49].

The present work is centered upon a new group of potassium antimonite vanadate glasses. Few studies have been made on glasses containing both Sb_2O_3 and V_2O_5 [18,50]. In most cases, they concern electrical, optical and magnetic properties. The potential application as oxygen sensor has been reported[36]. However, in these studies, V_2O_5 is a major component, or enters the glass matrix in smaller quantities for doping. Taking into account the large similarities between tellurite and antimonite glasses, it appears logical to investigate vitreous systems with Sb_2O_3 as the major glass former.

The starting point of the study is the combination of alkali vanadate and alkali antimonite glass. Potassium has been chosen as the alkali cation because we had evidence of vitreous KVO_3 . The other aim of the study is to quantify the influence of V_2O_5 on the physical properties.

2. Experimental

2.1 Glass preparation

These glasses were synthesized by conventional method. The starting materials used were:

- Antimony oxide Sb_2O_3 (Acros ~99%).
- Vanadium oxide V_2O_5 (Aldrich ~ 98%).
- Potassium carbonate K_2CO_3 (WWR-Merck

~99%).

Powders were mixed in appropriate proportions to yield about 10g in silica tubes. Then, the batch was melted at a temperature ranging from 700°C to 900°C for 10 min to obtain homogeneous and clear liquid. Finally, the melt was cooled at about 600 °C and cast in a brass mold preheated below the glass transition temperature T_g ($T_g - 20^\circ\text{C}$). Annealing was implemented at this temperature for 2 hours in order to minimize mechanical stress resulting from thermal gradients upon cooling. The glasses were finely polished using abrasive paper.

2.2 Physical measurements

Samples were subject to various physical measurements. X-ray diffraction patterns were collected at room temperature using $\text{Cu K}\alpha$ radiation on Philips PW 1830 diffractometer. Characteristic temperatures (T_g for glass transition, T_x for onset of crystallization and T_p for maximum of crystallization peak) were determined by differential scanning calorimetry (DSC) (Seiko DSC 220), the measurement error being smaller than 2°C. The heating rate was set to 10 $\text{K}\cdot\text{min}^{-1}$. The densities of glasses were determined by Archimedeian method using CCl_4 as an immersion liquid. Thermal expansion factor is measured in TMA/SS Seiko set-up using samples with thickness between 4 and 6mm. Infrared transmission spectra were recorded at room temperature using a BOMEM Michelson Spectrophotometer in the 400-4000 cm^{-1} range. The chemical composition of glasses has been checked by element analysis using energy dispersion spectrometry (Oxford link ISIS) set up incorporated into a JSM6400 Jeol scanning electron microscope.

3. Results

3.1. Vitreous domain

Glass forming area in the $\text{Sb}_2\text{O}_3\text{-V}_2\text{O}_5\text{-K}_2\text{O}$ ternary system is drawn in Fig. 1. It is limited by compositions corresponding to quenched glasses. Antimony oxide Sb_2O_3 forms binary glasses with the alkali oxide in the 20%-85% range, but only glass-ceramic and ceramics were obtained in the $\text{Sb}_2\text{O}_3\text{-V}_2\text{O}_5$ binary system. The $\text{V}_2\text{O}_5\text{-K}_2\text{O}$ binary system form glass in one single point -

50% Sb_2O_3 and 50% V_2O_5 - which corresponds to stoichiometric KVO_3 . Some of the ternary glasses are hygroscopic when alkali content is large.

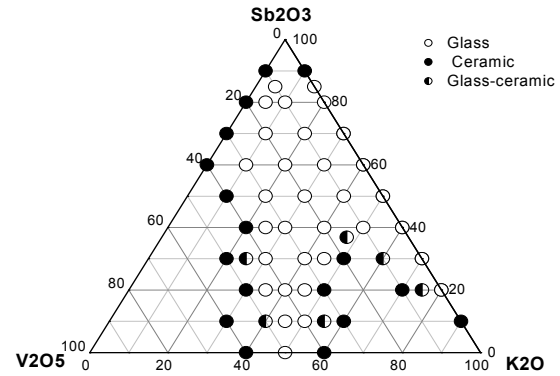


Fig.1. Phase diagram in the $\text{Sb}_2\text{O}_3\text{-V}_2\text{O}_5\text{-K}_2\text{O}$ ternary system (cast glasses).

In order to study the effect of V_2O_5 incorporation on glass properties, compositions were chosen with a constant percentage of alkali oxide K_2O . Thus a series of glass samples were prepared with the general formula: $(70-x)\text{Sb}_2\text{O}_3\text{-}x\text{V}_2\text{O}_5\text{-}30\text{K}_2\text{O}$. As vanadium content increases, their color gradually changes. Initially yellow, they turn green, brown, then darker and darker. Apart from the $70\text{Sb}_2\text{O}_3\text{-}30\text{K}_2\text{O}$ glass, they are stable at room atmosphere without surface alteration.

Typical diffraction patterns reproduced in Fig. 2 confirm the amorphous nature of the material and show no presence of crystalline phases.

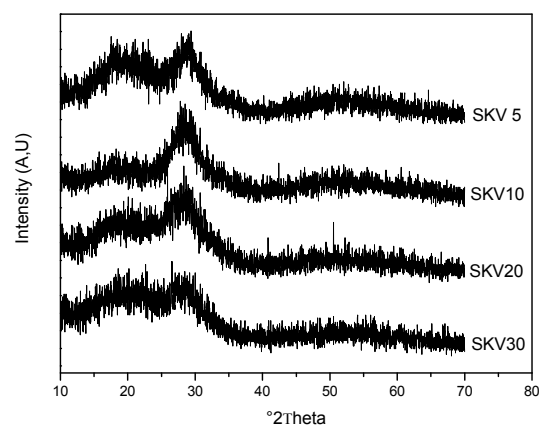


Fig.2. XRD pattern of $(70-x)\text{Sb}_2\text{O}_3\text{-}x\text{V}_2\text{O}_5\text{-}30\text{K}_2\text{O}$ glasses.

3.2. Thermal analysis

Characteristic temperatures were measured by DSC up to 500°C. They are reported in Table 1 and include the stability factor $\Delta T = T_x - T_g$ [51]. In most cases ($x \leq 30$)

crystallization peak is not observed, which means that crystallization does not occur at 10 K/min heating rate, as this appears in figure 3 for typical DSC curves. These data suggest that glasses from this system are very resistant against devitrification.

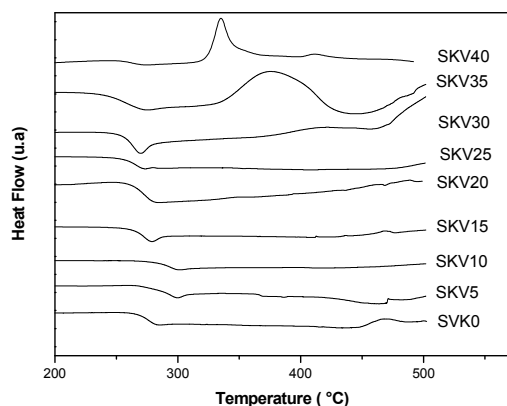


Fig. 3. DSC curves of glass samples in the $(70-x) \text{Sb}_2\text{O}_3$ $x\text{V}_2\text{O}_5$ $30\text{K}_2\text{O}$ system.

As one may expect, glass transition temperature T_g depends on chemical composition. A first set of measurements was carried out for increasing values of vanadium oxide concentration x . The general trend is that T_g decreases with increasing V_2O_5 content, from 284°C ($x = 5$) to 249°C ($x = 35$). Intriguingly, the evolution of T_g versus composition was not monotonous. In particular, T_g was lower than expected for $x = 0$ and higher for $x = 40$. The experimental values were confirmed by additional measurements and intermediate compositions were characterized ($x = 1, 2, 3, 4, 7, 33, 37$). As it appears in Fig. 4, T_g increases for $0 < x < 5$ and also for $x > 35$. This anomalous behavior should be explained in relation to glass structure.

Table 1. Characteristic temperatures. T_g is the temperature for glass transition, T_x for onset of crystallization, T_p for maximum of crystallization peak

Glass no	Sb_2O_3 (mol%)	K_2O (mol%)	V_2O_5 (mol%)	T_g ($^\circ\text{C}$)	T_c ($^\circ\text{C}$)	T_p ($^\circ\text{C}$)	ΔT ($^\circ\text{C}$)
SKV0	70	30	0	268	437	570	169
SKV5	65	30	5	284	-	-	-
SKV10	60	30	10	282	-	-	-
SKV15	55	30	15	273	-	-	-
SKV20	50	30	20	264	-	-	-
SKV25	45	30	25	246	-	-	-
SKV30	40	30	30	254	-	-	-
SKV35	35	30	35	249	453	473	204
SKV40	30	30	40	254	324	335	70

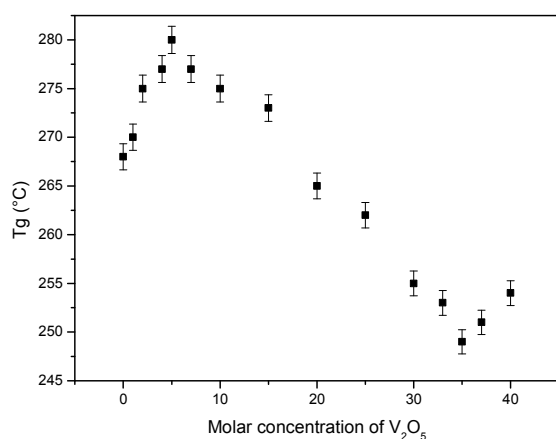


Fig. 4. Evolution of glass transition temperature versus V_2O_5 concentration.

Some glasses were analyzed by energy dispersion spectroscopy in a scanning electron microscope to compare their chemical composition from that of the batch. Only cations were considered as accuracy on

oxygen concentration is limited. In addition, the oxygen content is ruled by stoichiometry and can be deduced from that of cations. As this appears in Table 2 differences between the nominal and analyzed composition are small, which indicates that losses in the vapor phase during processing are limited. Silicium traces – less than 1 at % - originating from crucible material are observed in current samples.

Table 2. Nominal and EDS analyzed atomic compositions of the antimonite potassium vanadium glasses

x	Nominal			Analyzed		
	%Sb	%K	%V	%Sb	%K	%V
15	55	30	15	55.8	28.4	15.9
20	50	30	20	50.6	28.8	19.6
25	45	30	25	45.4	28.1	25.9
30	40	30	30	39.0	29.2	31.5
35	35	30	35	34.6	29.0	36.2

Concentration relates to 3 analyzed elements. Anionic oxygen is not taken into account. The relative uncertainty in EDS results is 1%.

3.3 Density

Density measurements have been implemented using the same series of glasses ($(70-x)\text{Sb}_2\text{O}_3 \cdot x\text{V}_2\text{O}_5 \cdot 30\text{K}_2\text{O}$). Results appear in figure 5: measured density decreases almost linearly versus V_2O_5 molar concentration. Limits of variation are 4.3 g cm^{-3} for vanadium free sample and 3.4 g cm^{-3} at 40 mol% V_2O_5 .

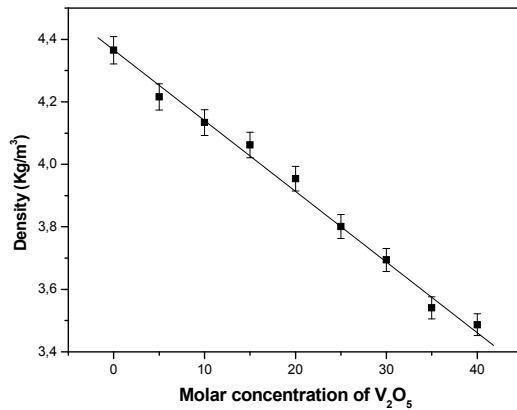


Fig.5. Variation of density with V_2O_5 concentration for $\text{Sb}_2\text{O}_3\text{-V}_2\text{O}_5\text{-K}_2\text{O}$ glasses. Line is drawn as a guide for eye.

3.4 Thermal expansion

Thermal expansion was measured in the $100 - 225 \text{ }^\circ\text{C}$ range for the same set of samples. The curve exemplifying the variation of the coefficient of thermal expansion (CTE) with V_2O_5 molar concentration (x) is shown in Fig. 6. The CTE grows for $0 < x < 25$, then it decreases for $x > 30$.

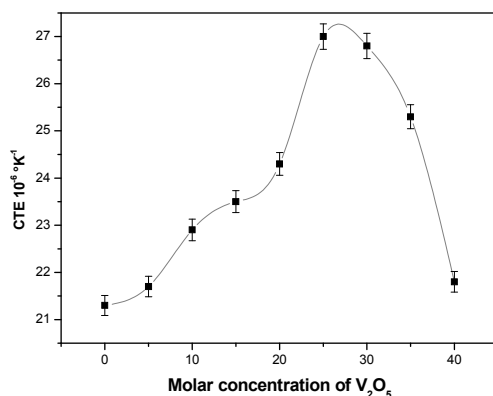


Fig.6. Evolution of Coefficient of Thermal Expansion versus V_2O_5 concentration. Line is drawn as a guide for eye.

3.5 Micro hardness and Elastic modulus

Microhardness is a bond sensitive property[52]. Yamane and Mackenzie[53] estimated the Vickers hardness number (VHN) of glasses from the relation,

$$\text{VHN} = C \sqrt{\alpha BG} \quad (1)$$

Where C is a constant, α is the bond strength factor, B is the bulk modulus and G is the shear modulus. The decrease in VHN with a decrease in the elastic modulus as predicted by relation (1) has been observed in many glasses [54,55] .

The microhardness and the elastic modulus of $(70-x)\text{Sb}_2\text{O}_3 \cdot x\text{V}_2\text{O}_5 \cdot 30\text{K}_2\text{O}$ glasses versus V_2O_5 content are reported in Figs. 7 and 8. They emphasize similar behaviors: the value of these physical properties first decreases with V_2O_5 content, reaching a minimum value at 25% V_2O_5 . Then it increases between 25% and 40% V_2O_5 .

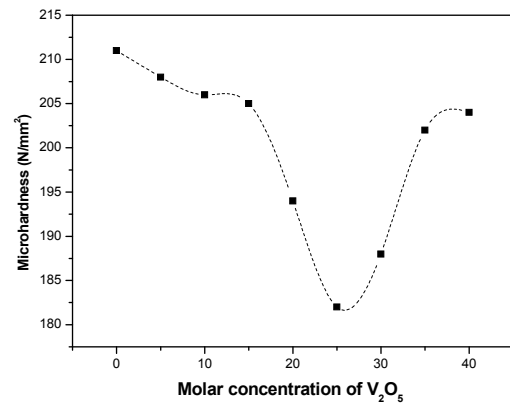


Fig.7. Evolution of micro hardness versus V_2O_5 concentration. Line is drawn as a guide for eye.

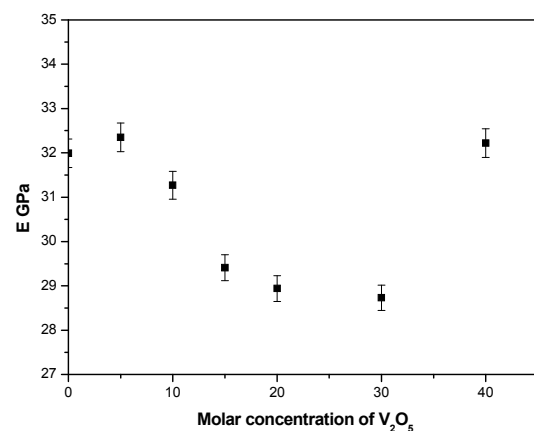


Fig.8. Variation of elastic modulus versus V_2O_5 concentration.

Microhardness is related to dilatometric softening point T_d [55], and it has been confirmed that microhardness of glasses decreases systematically with the decrease of the softening point T_d [56]. As the softening point relates closely to glass transition temperature T_g , the microhardness evolution is consistent with T_g measurements.

3. 6 Infrared transmission

Optical transmission of these glasses was recorded in the infrared spectrum. Typical transmission spectra are displayed in figure 9 for sample with increasing concentration in V_2O_5 . They show a large absorption band around 3000 cm^{-1} that originates from OH groups due to water contamination during processing. A second extrinsic absorption band is observed between 1700 and 1900 cm^{-1} . It corresponds to the first overtone of the fundamental Si-O vibration band at 984 cm^{-1} and arises from silicate anions from glass crucibles. The multiphonon absorption edge cannot be identified in these conditions.

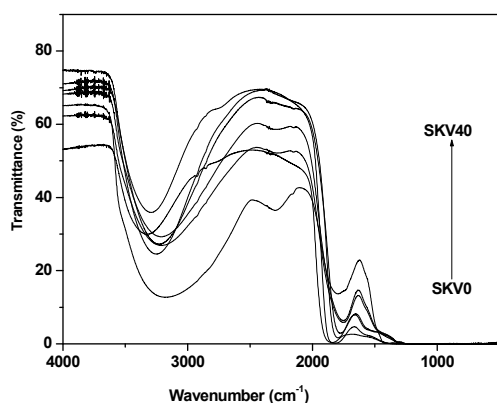


Fig. 9. Infrared transmittance of glass samples in the $(70-x)\text{Sb}_2\text{O}_3 \cdot x\text{V}_2\text{O}_5 \cdot 30\text{K}_2\text{O}$ system. Sample thickness: 1 mm .

4. Discussion

This vitreous system exhibits several interesting features. First, the glass forming range is very large, as it encompasses both vanadium-free and antimony-free compositions. This confirms the glass forming ability of Sb_2O_3 and V_2O_5 oxides. In a general way, the stability against devitrification decreases with increasing V_2O_5 content. Indeed, crystallization exotherm in DSC scans appears only for $x = 30$, while the thermal stability range T_x - T_g decreases from $204\text{ }^\circ\text{C}$ to $70\text{ }^\circ\text{C}$ when V_2O_5 concentration rises from 35 to 40 mol%.

Furthermore, the evolution of the physical properties versus composition has been studied in the $(70-x)\text{Sb}_2\text{O}_3$ - $x\text{V}_2\text{O}_5$ - $30\text{K}_2\text{O}$ series of glasses. Following a common rule, this evolution is expected to be linear as vanadium oxide substitute's antimony oxide. This is the case for

density that drops from 4.3 g cm^{-3} to 3.4 g cm^{-3} when x varies between 0 and 40. Density may be expressed as:

$$d = \frac{M}{V_m}$$

Where M is molar weight and V_m is molar volume. The composition rule leads to the linear decrease of M with vanadium concentration as molar weight of V_2O_5 is smaller than that of Sb_2O_3 (181.9 g vs 291.4 g). In the mean time, change in molar volume V_m should be small: in the crystalline state, molar volume of vanadium oxide is 54.3 cm^3 while it ranges from 51.4 to 56 cm^3 for antimony oxide, depending on the allotropic form. In these conditions, density is expected to decrease as this is observed. However V_m could vary in a non monotonous way, according to the Coordination Number (CN) of the Vanadium cation. The V_m variation results from the chemical formula (oxygen atoms are more numerous as V_2O_5 content increases) and also from the compactness change of the glass structure induced by CN change. This later effect is limited for two reasons: first V^{5+} cation is very small by comparison to oxygen anion; second, for both CN, the ratio of the cationic and anionic ionic radii [57] ($R(\text{V}^{5+})/R(\text{O}^{2-})$) is close to the ideal value of the close packing arrangement [58]. Therefore the structural changes described above do not alter the linearity of the density versus composition.

Surprisingly, the evolution is not monotonous for most other physical properties glass transition temperature such as micro hardness, elastic modulus, thermal expansion, and glass transition temperature. Additional and repeated synthesis and measurements confirmed it was not an artefact resulting from erratic factors in experiments. This behaviour cannot be explained simply as several parameters may influence these physical properties. For example, hardness relates to single bond strength while glass transition occurs when thermal motion leads to the breaking of chemical bonds. But global structure has also a significant effect: higher connectivity results in larger T_g and microhardness. Bond strength depends not only on the nature of the elements, but also on CN.

Therefore, one may think that changes in coordination numbers and connectivity explain the increase and the decrease of the physical parameters measured in the whole composition range. Crystal chemistry of vanadium is complex and rich [58]. The structure of vanadium (V) oxide V_2O_5 relates to that of Nb_2O_5 , but with some distortion: while NbO_6 octahedra are regular, vanadium cation shifts from the center of the octahedron, leading to a shorter V-O bond (1.6) and a longer one (2.8) by comparison to the four equatorial bonds (from 1.8 to 2). In this respect, CN may be viewed either as $5 + 1$ or 6 . The oxygen anion involved in the shorter V-O bond is also bonded loosely to second vanadium, forming the longer V-O bond. This longer bond is weaker, and therefore more sensitive to thermal motion. Vanadium tetrahedra are observed in alkali vanadates, and there are reports of VO_5 polyhedra in a few crystalline compounds such as

$\text{KVO}_3, \text{H}_2\text{O}$. Note that the octahedral coordination is classical for vanadium(IV): VO_2 has the rutile (TiO_2) structure. Sodium and potassium have high CN – up to 12 in perovskites- but it is often smaller: in the view of ionic radii[57], optimum compactness in oxides and fluorides corresponds to CN = 8. Antimony(III) oxide Sb_2O_3 is constructed from pyramidal units SbO_3 sharing corners and the same structural unit makes the basis of antimonite glasses[42]. This coordination polyhedron should rather be considered as a tetrahedron $\text{SbO}_3(\text{LP})$, in which LP is a lone pair of $5s^2$ electrons that occupies a volume similar to that of an oxygen anion. Table 3 gives the values of the single M-O bond energies of vanadium, antimony and potassium for current CNs. These values have been calculated by K. H. Sun as the ratio of dissociation energy and coordination number[59]. From this table, it appears that average V-O bond is stronger than Sb-O bond in VO_4 tetrahedra and smaller in VO_6 octahedra. The structure of the based glass $70\text{Sb}_2\text{O}_3\text{-}30\text{K}_2\text{O}$ may be described as the association of a $\text{Sb}_7\text{O}_{12}^{3-}$ network and 3 K^+ cations. Accordingly, there are 3 non bridging O- oxygen anions for 7 antimony cations in pyramidal units. When vanadium oxide substitutes antimony oxide, one may assume that SbO_3 groups are replaced by VO_4 tetrahedra, which gives one additional non-bridging oxygen per vanadium. Like in vitreous P_2O_5 this non-bridging oxygen does not bear any negative charge. The $\text{V}^{5+} / \text{Sb}^{3+}$ substitution raises the average bond strength, and consequently increases T_g . This mechanism may explain why T_g is larger for small additions of V_2O_5 . However, the reverse evolution is observed when V_2O_5 content exceeds 5 %! This suggests that a different mechanism takes place. It could involve a change in vanadium CN.

Table 3. Single bond strength F_b versus coordination number CN for K, Sb and V (59).

Cation	Charge(Z)	CN	F_b (Kcal/mol)
V	+5	4	112
V	+5	5	89
V*	+5	6	74
Sb	+3	3	78
K	+1	8	14

* Note that the longer V-O bond has a weaker energy.

There are obviously several possibilities and complementary characterizations are required to reach reliable assessments. Structural investigations may rely on vibrational spectroscopy (IR and Raman), ^{51}V MAS-NMR and X-ray absorption spectroscopy (XANES, EXAFS).

4. Conclusion

The investigation of the $\text{Sb}_2\text{O}_3\text{-V}_2\text{O}_5\text{-K}_2\text{O}$ ternary system has evidenced a large glass forming system that extends from Sb_2O_3 to KVO_3 . Some compositions appear very stable against crystallization. Characteristic temperatures, thermal expansion, density, micro hardness and elastic modulus have been measured. In particular, glasses with the $(70-x)\text{Sb}_2\text{O}_3\text{-}x\text{V}_2\text{O}_5\text{-}30\text{K}_2\text{O}$ composition allow to quantify the effect of the substitution of Sb_2O_3 by V_2O_5 in the $70\text{Sb}_2\text{O}_3\text{-}30\text{K}_2\text{O}$ base glass. The evolution of the physical properties versus vanadium content is not monotonous, with changes at 5 mol % and at 25-35 mol % V_2O_5 . This behavior is probably related to changes in coordination numbers of vanadium cations, and to network topology. This hypothesis should be confirmed by further structural investigations.

Acknowledgments

This work has been performed as a part of the « Programme Boursier Enseignants » of the Algerian Ministry of Higher Education and Scientist Research.

References

- [1] B. Aitken, M. Djeneke, Tungstate, molybdate, vanadate base glasses, U S Patent N° 6,376,399 B1, April 23, (2002)
- [2] A. Al-Hajri, A. Al-Shahrani, M. M. El-Desoky, Mater. Chem. Phys. **95**, 300 (2006)
- [3] O. Attos, M. Massot, M. Balkanski, E. Haro-Poniatowski, M. Asomawa, J. Non Cryst. Solids, **210** 163 (1997)
- [4] D. Bednarczyk, W. Chomka, O. Gzowski, XIV International Congress on Glass, New Delhi **2**, 96 (1986).
- [5] J. F. Bednarik, J. A. Neely, Glastech. Ber., **55**(6), 126 (1982)
- [6] D. Bersani, G. Antonioli, P. P. Lottici, Y. Dimitriev, V. Dimitrov, P. Kobourova, J. Non Cryst. Solids, **232-234**, 293 (1998)
- [7] V. Dimitrov, Y. Dimitriev, A. Montenero, J. Non Cryst. Solids, **180**(1), 51 (1994)
- [8] M. M. El-Desoky, J. Non Cryst. Solids, **351**, 3139 (2005).
- [9] M. M. El-Desoky, M. S. Al-Assiri, Mater. Sci. Engin., B **137**, 237 (2007)
- [10] M. D. Field, J. Appl. Phys., **40**, 2628 (1968)
- [11] G. N. Greaves, J. Non Cryst. Solids, **11**(5), 427 (1973).
- [12] S. Hayakawa, T. Yoko, S. Sakka, J. Non Cryst. Solids, **183**, 73 (1995)
- [13] B. Indrajit Sharma, P. S. Robi Srinivasan, Mater. Letters, **57**, 3504 (2003).
- [14] G. D. Khattak, N. Tabet, J. Electron Spectro. Rel. Phen., **136**, 257 (2004)
- [15] N. Krins, A. Rulmont, J. Grandjean, B. Gilbert, L.

- Lepot, R. Cloots, B. Vertruyen, *Solid State Ionics*, **177**, 3147 (2006).
- [16] J. M. Lewis, C. P. O'Brien, M. Affatigato, S. A. Feller, *J. Non Cryst. Solids*, **293-295**, 663 (2001)
- [17] A. Mekki, G. D. Kattak, L. E. Wenger, *J. Non Cryst. Solids*, **330**, 156 (2003)
- [18] H. Mori, T. Kitami, H. Sakata, *J. Non Cryst. Solids*, **168** (1-2), 157 (1994).
- [19] C. Narayana Reddy, V. C. Veeranna Gowda, R. P. Sreekanth Chakradhar, *J. Non Cryst. Solids*, **354** 32 (2007).
- [20] A. Nicula, E. Culea, I. Lupsa, *J. Non Cryst. Solids*, **79**(3), 325 (1986)
- [21] V. Rajendran, N. Palanivelu, B. K. Chaudhuri, K. Goswami, *J. Non Cryst. Solids*, **320**, 195 (2003)
- [22] K. V. Ramesh, D. L. Sastry, *J. Non Cryst. Solids*, **325** 5421 (2006)
- [23] K. V. Ramesh, D. L. Sastry, *Mater. Sci. Engin.*, **B 126**, 66 (2006)
- [24] S. Sen A. Ghosh, *J. Non Cryst. Solids* **258**, 29 (1999)
- [25] S. Sen A. Ghosh, *J. Mater. Res.*, **15**(4), 995 (2000)
- [26] M. A. Sikdey R. El Mallawany, *J. Non Cryst. Solids*, **215**, 75 (1997).
- [27] S. Sindhu, S. Sanghi, A. Agarwal, N. Kishore, V. P. Seth, *J. Alloys Comp.*, **428**, 206 (2007)
- [28] V. Sudarsan S. K. Kulshreshtha, *J. Non Cryst. Solids*, **258**, 20 (1999).
- [29] S. Szu, F.-S. Chang, *Solid State Ionics*, **176**, 2696 (2005)
- [30] N. Tashtoush, A. Qudah, M. M. El-Desoky, *J. Phys. Chem. Solids*, **68**, 1926 (2007).
- [31] G. Tricot, L. Montagne, L. Delevoye, G. Palavit, V. Kostoj, *J. Non Cryst. Solids*, **345-346**, 56 (2004)
- [32] W. H. Zachariasen, *J. Amer. Chem. Soc.*, **54**, 3841 (1932).
- [33] S. Hayakawa, T. Yoko, S. Sakka, XVII International Congress on Glass, Beijing, Chinese Ceramic Society, **2** 177 (1995)
- [34] A. Abd El-Moneim, *Mater. Chem. Phys.*, **73**, 318 (2002)
- [35] R. El-Mallawany, *Mater. Chem. Phys.*, **63**, 109 (2000)
- [36] H. Mori, H. Sakata, *Mater. Chem. Phys.*, **45**, 211 (1996)
- [37] E. Kordes, *Z. Phys. Chem.*, **B43**, 173 (1939)
- [38] A. Winter, *Verres et Réfract.*, **9**, 147 (1955)
- [39] A. Winter, *Verres Réfract.*, **36** (2), 353 (1982)
- [40] M. T. Soltani, A. Boutarfaia, R. Makhloufi, M. Poulain, *J. Phys. Chem. Solids*, **64**(12), 2307 (2003)
- [41] B. Dubois, H. Aomi, J. J. Videau, J. Portier, P. Haggemuller, *Mat. Res. Bull.*, **19**, 1317 (1984)
- [42] B. Dubois, J. J. Videau, M. Couzi, J. Portier, *J. Non Cryst. Solids*, **88**, 355 (1986)
- [43] M. Nalin, M. J. Poulain, M. A. Poulain, S. Ribeiro, Y. Messaddeq, *J. Non Cryst. Solids*, **284**, 110 (2001)
- [44] G. Poirier, M. A. Poulain, M. J. Poulain, *J. Non Cryst. Solids*, **284**, 117 (2001)
- [45] M. Legouera, P. Kostka, M. Poulain, *J. Chem. Phys. Solids*, **65**, 901 (2004)
- [46] N. F. Mott, *J. Non Cryst. Solids*, **1**, 427 (1968)
- [47] S. Kim, T. Yoko, S. Sakka, *J. Am. Ceram. Soc.*, **76**, 805 (1993)
- [48] E. De Araujo, C. B. De Araujo, G. Poirier, M. Poulain, Y. Messaddeq, *Appl. Phys. Lett.*, **8**(25), 4694 (2002).
- [49] A. Mori, K. Kobayashi, M. Yamada, T. Kanamori, K. Oikawa, Y. Nishida, Y. Ohishi, *Electron. Lett.*, **34**(9), 887 (1998)
- [50] M. Amano, K. Suzuki, H. Sakata, *J. Mater. Sci.*, **32**, 4325 (1997)
- [51] A. Dietzel, *Glastech. Ber.*, **22**(7), 41 (1968)
- [52] J. Zarzycki, *Materials Science and Technology*, Vol.9, Weinheim, New York, 1991
- [53] M. Yamane, J. D. Mackenzie, *J. Non Cryst. Solids*, **15**(2), 153 (1974)
- [54] A. Petzold, F. G. Withsmann, H. Von Kampiz, *Glastech. Ber.*, 43 (1961).
- [55] J. E. Shelby, *Introduction to Glass Science and Technology*, Royal Soc. Chem., Cambridge, 1997
- [56] A. R. Hilton, C. E. Jones, M. Baru, *Phys. Chem. Glasses*, **7**, 105 (1966)
- [57] R. D. Shannon, *Acta Cryst.*, **A32**, 751 (1976)
- [58] A. F. Wells, *Structural Inorganic Chemistry*, Clarendon Press, Oxford, 1975
- [59] K. H. Sun, *J. Am. Ceram. Soc.*, **30**(9), 277 (1947)

*Corresponding author: marcel.poulain@univ-rennes1.fr